NUMERICAL SIMULATION OF INTERNAL FLOW IN A LARGE-SCALE PRESSURE-SWIRL ATOMIZER

Jesper Madsen, Bjørn H. Hjertager, Tron Solberg

Aalborg University Esbjerg, Niels Bohrs Vej 8, DK-6700 Esbjerg, Denmark
E-mail: jema@aue.auc.dk, bhh@aue.auc.dk, tron@aue.auc.dk

ABSTRACT

This work is a continuation of experimental and computational studies of the internal flow field of a large-scale Danfoss atomizer presented at an earlier ILASS conference [1,2]. Fluent 6.1 is used to simulate the flow through the large-scale atomizer. The two-phase flow is modeled using three approaches: 1) a volume of fluid (VOF) method using a laminar flow assumption, 2) a VOF method using large eddy simulation (LES) turbulence modeling, and 3) a two-fluid Euler/Euler method using a laminar flow assumption. The primary focus of the analysis is on the internal flow characteristics in the swirl chamber. The air/water flow inside the atomizer is determined for two volume flow rates. Where possible, comparisons are made with measured velocity profiles and photographs of the air-core and the spray-cone from the atomizer. The CFD results compare favorably with experimental data of tangential and axial velocity distributions in the swirl chamber and static wall pressure. The size and shape of the air-core is also captured well by the numerical simulations.

1 INTRODUCTION

Pressure-swirl atomizers producing hollow cone fuel sprays are commonly used in oil-fired boilers because they produce good atomization characteristics and are relatively simple and inexpensive to manufacture. To ensure a good combustion, it is critical to design atomizers that can produce sprays with a predetermined droplet size distribution at the desired combustor locations. Therefore, prediction of the atomizer performance for design and analysis is critical. Currently, semi-empirical correlations are used to provide guidance in designing pressure-swirl atomizers. Lefebvre [3] provides a detailed review of the experimental and theoretical studies on the flow phenomena in atomizers and spray formation.

One way to study internal flows in atomizers is to use large-scale models in experimental investigations. Studies reported by [4-8] used large-scale pressure-swirl atomizers to enable measurements of air-core size and velocity fields inside the swirl chambers and orifices of the atomizers. Such studies are difficult to perform for production-scale atomizers.

As a compliment to the limitations of the experimental techniques, computational fluid dynamics (CFD) provide additional insight into the dynamics of the internal flow of pressure-swirl atomizers. However, when applying CFD in a new way to model fluid-dynamic behavior, some form of validation is necessary for reliable results. The main difficulty in the numerical simulation of the flow in a pressure-swirl atomizer is the accurate tracking of the liquid/air interface. Jeng, *et al.* [4] and Sakman, *et al.* [9] performed two-dimensional turbulent numerical simulations using moving grids for representing the free surface. Yule and Chinn [7] used Fluent to solve for the liquid flow field. They determined the position of the interface with an approximate method and restricted their simulation to laminar flow. Steinthorsson and Lee [10] used the Volume of Fluid (VOF) method in Fluent 5 to simulate three-dimensional flow, while a Reynolds stress model was used to model turbulence. More recently, von Lavante, *et al.* [11] performed numerical simulations of internal flow in both two- and three-dimensional models using the VOF-method, and Buelow, *et al.* [12] used a two-phase VOF technique to simulate the flow through a small-scale pressure-swirl atomizer.

Hansen and Madsen [1,2] performed both experimental and computational studies of a large-scale pressure-swirl atomizer. The atomizer used in this study was scaled up from a production scale Danfoss atomizer. The atomizer shown in Fig. 1 (a) was manufactured form Plexiglas. This atomizer had a different geometry than used in the references [4-11]. Three feed slots were positioned on top of a conical swirl chamber, which lead to the outlet via a cylindrical orifice. The top diameter of the swirl chamber was 100 mm and the length was 40 mm. The orifice had a diameter of 20 mm and a length of 30 mm. The experimental values of tangential and axial velocity were obtained using laser Doppler anemometry. Radial profiles of axial and tangential velocities at five axial locations in the swirl chamber were measured. The gas-liquid flow was simulated using the homogeneous two-phase model in CFX-4.3.

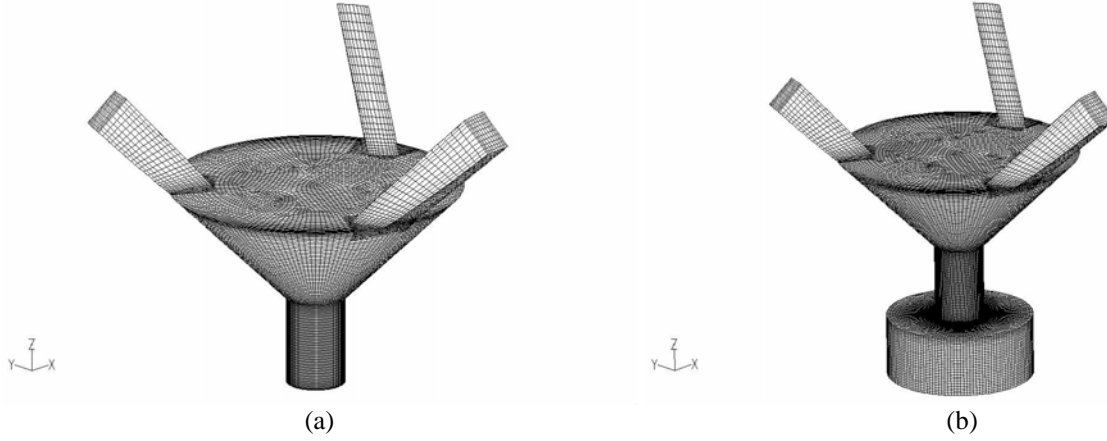<div align="center">(a)</div> <div align="center">(b)</div>

Fig. 1. Grid consisting of three feed slots, swirl chamber, and orifice.
(a) internal domain and (b) internal and near-field spray-cone domains.

The flow-field was simulated using both a laminar flow assumption and large eddy simulation (LES) turbulence modeling. It was found that the CFD models could capture the features of the internal flow of the atomizer. Trends of tangential velocity were predicted very well by the CFD model; however, magnitudes were under-predicted. Some of this discrepancy may be due to the grid used for the numerical simulations. The flow field was computed on a three-dimensional structured grid; however, the three feed slots were not included in the model, and therefore, the interaction between the feed slots and the swirl chamber was not captured.

In the present study, Fluent-6.1 is used to simulate the flow through the large-scale atomizer investigated by Hansen and Madsen [1,2]. The primary focus of the analysis is on the internal flow characteristics in the swirl chamber, the resulting liquid film properties at the exit of the atomizer as well as the near-field spray-cone prior to film breakup. Where possible, comparisons are made with measured velocity profiles and photographs of the air-core and the spray-cone from the atomizer.

2 NUMERICAL METHODS

Two grids are constructed for the present study. Initially, the numerical simulations are performed using a three-dimensional grid of hexahedral, tetrahedral and prismatic cells, consisting of the three feed slots, the conical swirl chamber, and the cylindrical orifice; see Fig. 1 (a). The tetrahedral and prismatic cells are located in the swirl camber downstream the feed slots; the remaining cells are all hexahedral. Furthermore, cells are tightly spaced near the walls. When the solution is near steady state, the mesh around the fluid interface is refined. This allows sharp velocity gradients and the interface itself to be captured more sharply. The original grid consists of 297,446 cells and the adapted consists of about 600,000 cells.

The second grid includes the three feed slots, the swirl chamber, the orifice, and the near field spray-cone 25 mm downstream the atomizer; see Fig. 1 (b). This grid is constructed to model the liquid film cone exiting from the atomizer. As described above, the mesh around the interface is refined. The original grid consists of 553,549 cells, and the adapted of about 1.1 million cells.

Three approaches described below are used for the two-phase flow simulations.

2.1 Volume of Fluid (VOF) Model

Many methods exist to simulate two-phase flow-fields and a brief examination of the currently available techniques can be found in Steinthorsson and Lee (2000) [10]. In this study, the VOF method, implemented in the commercially available CFD code Fluent-6.1, is used to simulate the flow of water and air in the large-scale pressure-swirl atomizer. For each phase that is modeled, a volume fraction for that phase is determined in each cell by the solution of a transport equation. When the volume fraction is between zero and one, there exists a fluid interface within the computational cell. The volume fraction equation can be solved using standard upwind differencing techniques, which tend to smear the surface over a few cells, or by Geometric Reconstruction of the two-phase interface, which ensures that the two-phase boundary is captured within one computational cell [13]. In this work the Geometric Reconstruction scheme computed in a time-accurate manner is used to keep the interface sharp.

2.2 Large Eddy Simulation (LES) Model

In the light of the fact that the Reynolds number for this flow-field is in the order of 12,000 to 41,000 (based on the conditions in the feed slots and the hydraulic diameter of the feed slots), the flows within the feed slots and swirl chamber may be turbulent. It was attempted to make use of the standard, the RNG, and the realizable two-equation k-ε turbulence models in Fluent-6.1. However, for this particular flow-field the turbulence models were unable to predict the air-core. Therefore, the flow-field is simulated using both a laminar flow assumption and LES turbulence modeling.

In the LES methodology one solves only those eddies that are large enough to contain information about the geometry and dynamics of the specific problem under investigation, and regards all structures on a smaller scale as "universal" following the viewpoint of Kolmogorov. The LES equations are derived by applying a filter function to the time-dependent Navier-Stokes equations. While LES of mono-phase flows has reached a sophisticated standard, applications of LES formalism to two-phase flows with moving interfaces are harder to find in the literature. A concern for two-phase simulations is the ability to correctly model the turbulence in the presence of liquid and air. In this work, the standard Smagorinsky-Lilly [14,15] model is considered. The influence of the unresolved motion on the resolved scales is treated as an additional viscosity, μ_t, modeled by

$$\mu_t = \rho L_S^2 \sqrt{2\overline{S}_{ij}\overline{S}_{ij}} \tag{1}$$

where $\overline{S}_{ij}$ is the rate-of-strain tensor for the resolved scale and L_S is the mixing length for subgrid-scales computed using

$$L_S = \min\left(\kappa d_w, C_S V^{1/3}\right) \tag{2}$$

where κ is the von Kármán constant, d_w is the distance to the closest wall, and V is the volume of the computational cell. C_S is the Smagorinsky constant and a value of $C_S = 0.1$ is used.

The work represents a first step in applying LES in a VOF simulation, and the issue of additional terms due to the interface is not considered.

2.3 Two-Fluid Euler/Euler Model

In a later stage of the study a multiphase Eulerian modeling approach will be used to predict the downstream film breakup behavior. Instead of switching from a VOF method inside the atomizer to an Eulerian multiphase method downstream the nozzle, a two-fluid Euler/Euler method is considered for the flow inside the atomizer also.

The Eulerian multiphase approach treats the liquid and air as separate interpenetrating phases. For each phase mass and momentum equations are solved as well as an equation for volume fraction. In this study, momentum exchange between the gas and liquid is modeled through a symmetrical drag model. The gas-liquid momentum exchange coefficient, C_{gl}, is written in terms of mixture density, ρ_{gl}, and mixture interfacial area density, A_{gl}:

$$C_{gl} = \frac{1}{8} C_D \rho_{gl} A_{gl} \left| \vec{u}_g - \vec{u}_l \right| \tag{3}$$

where

$$\rho_{gl} = \alpha_g \rho_g + \alpha_l \rho_l \text{ and } A_{gl} = \frac{6\alpha_g \alpha_l}{d_{gl}} \tag{4}$$

where $d_{gl} = \alpha_g d_l + \alpha_l d_g$ is an interfacial length scale, α_g and α_l are the volume fraction of gas and liquid, d_g and d_l are the diameter of bubbles and droplets. For this first step a value of $d_g = d_l = 1.0$ mm is used.

The drag coefficient, C_D, is based on the Schiller-Naumann and Newton particle drag correlations:

$$C_D = \max\left[\frac{24}{\mathrm{Re}_{gl}} \left(1 + 0.15\mathrm{Re}_{gl}^{0.687}\right), 0.44 \right] \tag{5}$$

where Re_{gl} is the relative mixture Reynolds number obtained from:

$$\mathrm{Re}_{gl} = \frac{\rho_{gl} \left| \vec{u}_g - \vec{u}_l \right| d_{gl}}{\mu_{gl}} \tag{6}$$

where $\mu_{gl} = \alpha_g \mu_g + \alpha_l \mu_l$ is the mixture viscosity of gas and liquid. This symmetrical drag model gives correct behavior for particle flow with vanishing volume fractions.

3 RESULTS

The flow simulations are done for the two geometries shown in Fig. 1. The boundary condition for the inlets is taken to be a specified volume flow rate normal to the boundary. The downstream pressure boundary is set to ambient pressure (101325 Pa), All wall boundaries are taken as no-slip. For all cases, the fluids are air and water at an operating temperature of 50°C. For air and water respectively, the densities are 1.04 and 988 kg/m^3, the viscosities are 1.84×10^{-5} and 5.44×10^{-4} kg/m s, and surface tension is 0.068 N/m.

Two operating conditions are computed, with water volume flow rates of 15 and 50 L/min, respectively. The simulations are run as time-dependent, and the time steps used for the two cases are 1.0×10^{-4} and 2.5×10^{-5} s, respectively. The choice of the time-step interval used in the computations is based on a Courant number of 1, and it was found that these intervals were sufficient to display the time dependency and to ensure convergence for each time step. Obtaining a converged steady-state solution was found to be impossible.

In both of the VOF cases and the Two-Fluid case, the interface between the liquid and the gas become unsteady, displaying waves of small magnitude along its surface; see Fig. 2. The waves originate at the atomizer top, at the stagnation point on the wall, and propagate toward the exit. The stagnation point leads to the formation of a crest at the atomizer top. The resulting flows are of highly three-dimensional character, where the air-core is rotating, generating a spiraling disturbance on its surface. The qualitative agreement of the experimentally obtained flow visualization data in [1,2] with the present numerical simulations is good. For both flow rates the air-core has a near-constant mean diameter throughout the conical swirl chamber. Over a distance of approximately 10 mm in the cylindrical orifice, the air core is seen to expand to a second near-constant mean diameter. The drawback to the Two-Fluid approach is that the interface is poorly resolved compared to the VOF approaches. Therefore, the volume fraction and velocity gradients become smeared over a few cells.

The velocity and thickness of the liquid film at orifice exit, as well as the downstream variations, are of interest because they govern the breakup of the film. Unfortunately, grid resolution requirements for the VOF simulation restrict the simulation to 25 mm downstream from the exit of the atomizer, see Fig. 2. The liquid film thins out so rapidly that an additional 2-3 million cells within the film would be required to resolve the film. However, the CFD model does provide adequate grid resolution to resolve the liquid film in the orifice and at the exit of the atomizer. The film properties here are important, because they can provide the boundary conditions for film breakup models.

In the experiments [1,2], the tangential velocity profiles in the conical swirl chamber were found to be essentially independent of the axial position. This is also found in the simulations. The velocity distributions in the swirl chamber are similar for both grids in Fig. 1. For the region close to the orifice exit, the results show little difference between the two grids. This suggests that the downstream flow field only affects the internal flow filed of the atomizer in a region close to the exit. In the figures in this paper the results are plotted for the grid in Fig. 1 (a).

Fig. 3 shows a comparison of tangential velocity measurements and predictions at an axial position 10 mm below the top of the swirl chamber, with volume flow rates of 15 and 50 L/min. The general agreement between the measured and the three present cases (VOF, VOF-LES, and Two-Fluid) is good. It is seen that the tangential velocity component exhibits the $1/r$ variation for the irrational region of a free vortex for most of the chamber width. The flow simulations carried out in [1,2] using CFX-4.4 and the assumption of laminar flow (CFX-lam) deliver similar qualitative behavior; however, the tangential velocity is under-predicted by as much as 20-40%. This under-prediction is due to the grid used where the three feed slots were not included in the model, and therefore, the interaction between the feed slots and the swirl chamber was not captured.

Fig. 4 shows mean axial velocity at an axial position 10 mm below the top of the swirl chamber. Both the present computations and measurements show that the axial component of the velocity is concentrated within a region surrounding the air-core, and in this region this gives a deviation in the tangential velocity profile from the free vortex shape. A peak in axial velocity is also seen next to the wall at $r = 0.4$ mm, and everywhere else both the axial and radial velocities are very small compared with the tangential. Between the wall and the air-core the axial velocity contains both positive and reverse flow. The negative peaks in axial velocity profile near the air-core and next to the wall are not obtained in the CFX results.

Fig. 5 compares the predicted and measured static wall pressures for the two flow rates, and there is seen to be generally good agreement between the present predictions and experiment. The computed pressures using CFX are 40-50% lower than the measured. This discrepancy is due to the under-prediction of tangential velocity.

The VOF and Two-Fluid approaches assuming laminar flow deliver very similar results comparing velocity profiles and static wall pressure, while the LES approach dampens the flow and reduces the static wall pressure. The best general agreement is seen for the laminar flow approaches, indicating laminar flow in the swirl chamber. The drawback to the Two-Fluid approach is that the interface becomes smeared over a few cells, and due to the extra set of momentum equations and more iteration needed per time step, it requires more computation time. Therefore, the results of this study suggest that the use of VOF modeling assuming laminar flow is the best choice for the cases examined here.
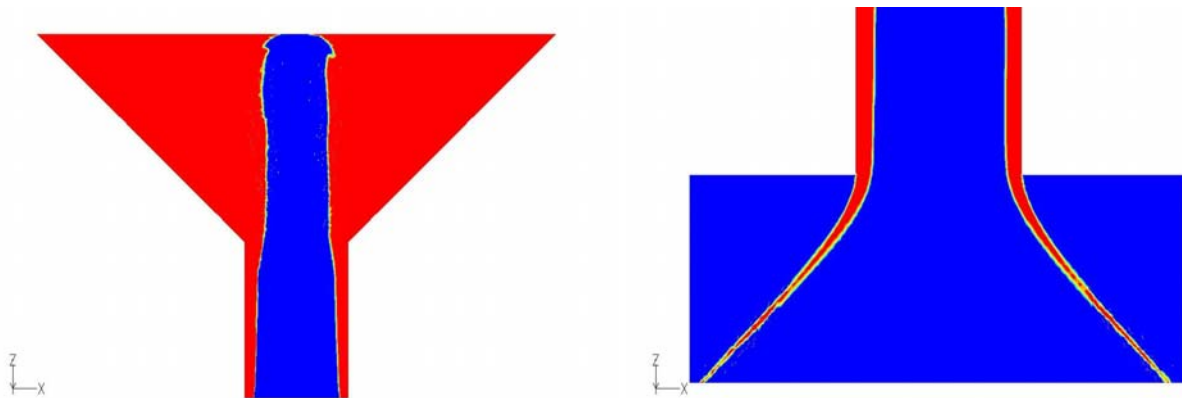

Fig. 2. Contours of volume fraction for the VOF case at 50 L/min (water in red and air in blue)
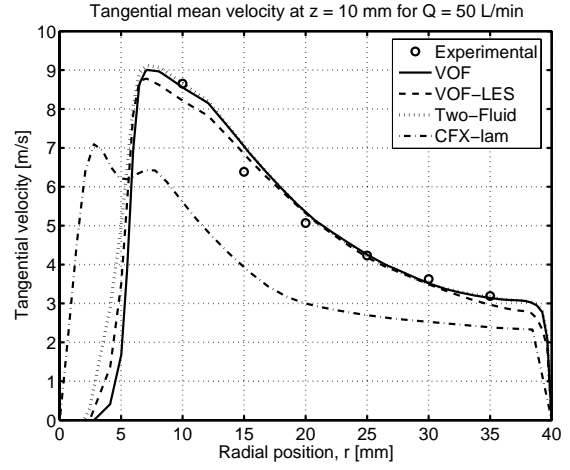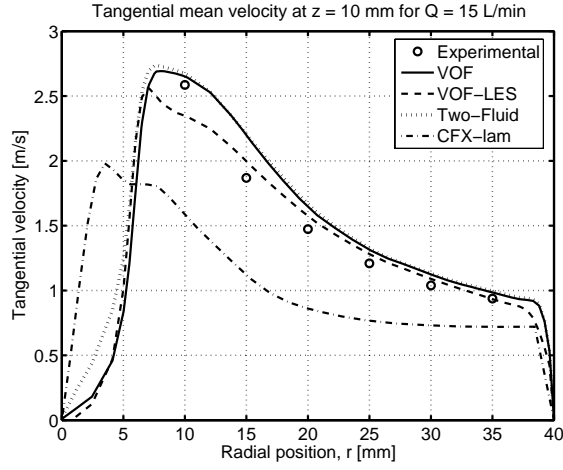for the internal domain (left) and the near field spray-cone (right).

Fig. 3. Comparison of mean tangential velocity profiles for flow rate of 15 L/min (left) and 50 L/min (right) at an axial position 10 mm below the top of the swirl chamber.
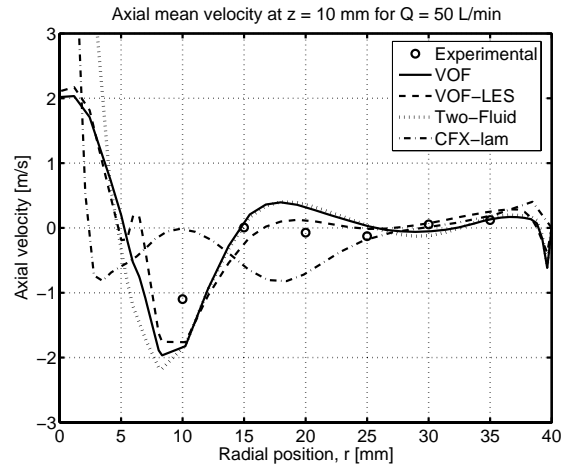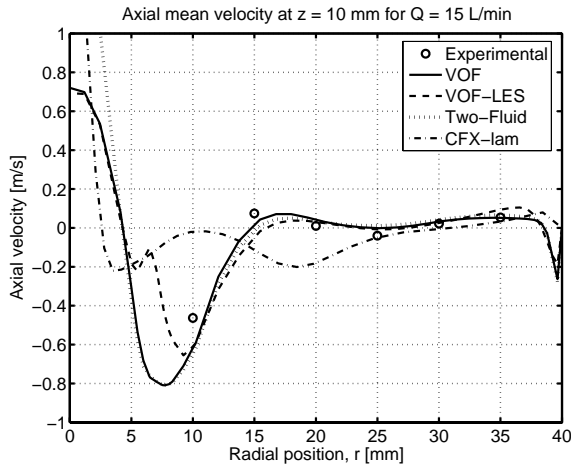

Fig. 4. Comparison of mean axial velocity profiles for flow rate of 15 L/min (left) and 50 L/min (right) at an axial position 10 mm below the top of the swirl chamber.
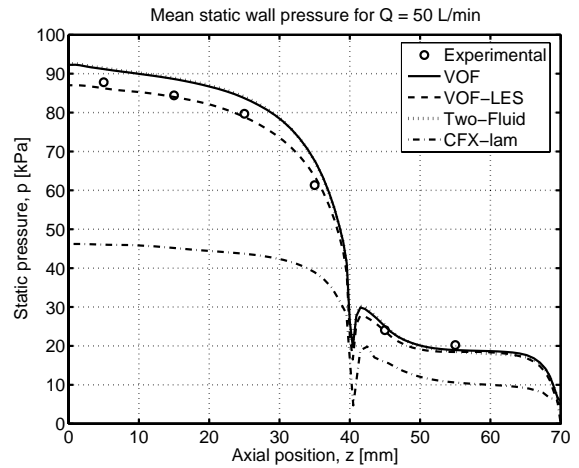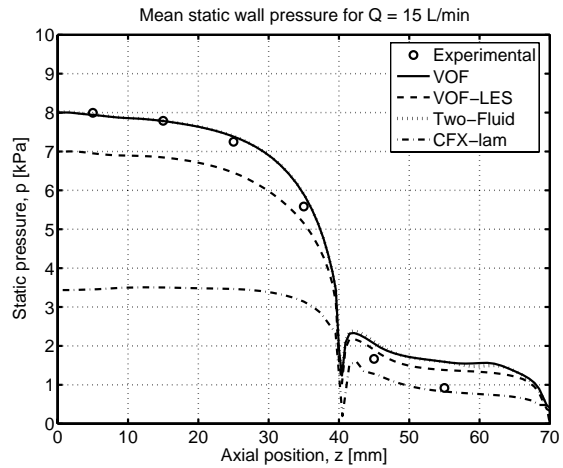

Fig. 5. Computed and measured mean static wall pressure (gauge) for flow rate of 15 L/min (left) and 50 L/min (right).

4 CONCLUSIONS

The applicability of two-phase CFD modeling of the internal flow in a large-scale pressure-swirl atomizer is investigated using three approaches: 1) a VOF method using a laminar flow assumption, 2) a VOF method using LES turbulence modeling, and 3) a two-fluid Euler/Euler method using a laminar flow assumption. All simulations deliver similar results and produce the characteristic air-core that matches those observed in the experiments. Likewise, tangential and axial velocity profiles in the conical swirl chamber and static wall pressure are found to match favorably with the measured profiles. For the two flow rates considered here, the VOF and Two-Fluid approaches assuming laminar flow appear to give the best agreement.

For more accurate predictions, some refinements of the approaches are needed. For instance, finer mesh may be needed, and a refinement in the LES model may be needed to capture the turbulence in presence of the liquid/air interface correctly. The ability of the two-fluid model to predict the flow-field should also be further assessed, especially the drag correlation and the two diameters d_g and d_l.

The liquid film cone exiting from the atomizer is modeled in a region 25 mm downstream the atomizer prior to film breakup. The atomizer and near-field spray-cone is simulated using 1.1 million cells; however, the resolution is insufficient. To include the breakup of the liquid film, an even finer grid resolution would be required.

In future work, CFD modeling will be used to predict the internal flow-field of production-scale pressure-swirl atomizers and twin-fluid Y-jet atomizers, and a multi-phase Eulerian modeling approach will be used to predict the downstream film breakup behavior and the dispersion of the spray.

ACKNOWLEDGEMENTS

NOMENCLATURE

A_{gl}	interfacial area density	$[\text{m}^2/\text{m}^3]$
C_D	drag coefficient	$[-]$
C_{gl}	friction coefficient	$[\text{kg/m}^3\,\text{s}]$
C_S	Smagorinsky constant	$[-]$
d	diameter	$[\text{m}]$
d_w	wall distance	$[\text{m}]$
L_S	subgrid length scale	$[\text{m}]$
p	pressure	$[\text{Pa}]$
Q	volume flow rate	$[\text{m}^3/\text{s}]$
r	radial position	$[\text{m}]$
Re	Reynolds number	$[-]$
$\overline{S}_{ij}$	rate-of-strain tensor	$[\text{s}^{-1}]$
$\vec{u}$	velocity vector	$[\text{m/s}]$
V	volume	$[\text{m}^3]$
z	axial position	$[\text{m}]$

Greek Symbols

α	volume fraction	$[-]$
κ	von Kármán constant	$[-]$
μ	viscosity	$[\text{kg/m s}]$
ρ	density	$[\text{kg/m}^3]$

Subscripts

g	gas
gl	mixture
l	liquid
S	subgrid
t	turbulent

REFERENCES

1. K.G. Hansen, J. Madsen, C.M. Trinh, C.H. Ibsen, T. Solberg and B.H. Hjertager, A computational and experimental study of the internal flow in a scaled pressure-swirl atomizer, *Proc. ILASS-Europe 2002*, 2002.
2. K.G. Hansen and J. Madsen, A Computational and Experimental Study of the Internal Flow in a Scaled Pressure-Swirl Atomizer, M.Sc. thesis, Aalborg University Esbjerg, Denmark, 2001.
3. A.H. Lefebvre, *Atomization and Sprays*, Hemisphere, New York, 1989.
4. S.M. Jeng, M.A. Jog and M.A. Benjamin, Computational and experimental study of liquid sheet emanating from simplex fuel nozzle, *AIAA Journal*, vol. 36, pp. 201-207, 1998.
5. D. Cooper, A.J. Yule and J.J. Chinn, Experimental measurements and computational predictions of the internal flow field in a pressure swirl atomizer, *Proc. ILASS-Europe '99*, 1999.
6. Z. Ma, D. Wang, S.-M. Jeng and M.A. Benjamin, On the internal flow of pressure-swirl atomizer at two different density ratios, *Proc. ICLASS 2000*, p. 1206, 2000.
7. A.J. Yule and J.J. Chinn, The internal flow and exit conditions of pressure swirl atomizers, *Atomization and Sprays*, vol. 10, pp. 121-146, 2000.
8. D. Cooper and A.J. Yule, Waves on the air core/liquid interface of a pressure swirl atomizer, *Proc. ILASS-Europe 2001*, 2001.
9. A.T. Sakman, M.A. Jog, S.M. Jeng and M.A. Benjamin, Parametric study of simplex fuel nozzle internal flow and performance, *AIAA Journal*, vol. 38, pp. 1214-1218, 2000.
10. E. Steinthorsson and D.M. Lee, Numerical simulations of internal flow in a simplex atomizer, *Proc. ICLASS 2000*, p. 324, 2000.
11. E. von Lavante, U. Maatje and F.-O. Albina, Investigation of unsteady effects in pressure swirl atomizers, *Proc. ILASS-Europe 2002*, 2002.
12. P.E.O. Buelow, C.-P. Mao and S. Smith, Two-phase CFD modeling of a simplex atomizer, *Proc. ILASS-Americas 2003*, 2003.
13. Fluent, *Fluent 6.1 User's Guide*, Fluent Inc., Lebanon, NH, 2003.
14. J. Smagorinsky, General circulation experiments with the primitive equations. I. The basic experiment, *Monthly Weather Review*, vol. 91, pp. 99-165, 1963.
15. D.K. Lilly, The representation of small-scale turbulence in numerical simulation experiments, *Proc. IBM Scientific Computing Symposium on Environmental Sciences*, pp. 195-210, 1967.